Annals of Nuclear Energy 224 (2025) 111733

Contents lists available at ScienceDirect

Annals of Nuclear Energy

journal homepage: www.elsevier.com/locate/anucene

Assessment of radionuclide dispersion and radiation dose for a hypothetical VVER-1200 accident in Zimbabwe

S. Chiyangwa [a,*], S.A. Birikorang [b], V.Y. Agbodemegbe [c]

[a] Solomon Chiyangwa, Radiation Protection Authority of Zimbabwe, 160 Baines Avenue, Harare, Zimbabwe
[b] Nuclear Regulatory Authority, House 1&2, Neutron Avenue, P. O. Box AE 50, Atomic Energy, Accra, Ghana
[c] Graduate School of Nuclear and Allied Sciences, College of Basic and Applied Sciences, University of Ghana, P.O. Box AE1, Atomic Energy, Accra, Ghana

ARTICLE INFO

Keywords:
LOCA
Source term
TEDE
CTCED
PAGs VVER-1200
Radiological safety
Loss of Coolant Accident (LOCA)
RASCAL 4.3.4
Total Effective Dose Equivalent (TEDE)
Potassium iodide (KI)
Meteorological data
Containment leakage

ABSTRACT

The potential introduction of a VVER-1200 nuclear reactor in Zimbabwe to meet the growing energy demands requires a thorough understanding of its radiological safety and environmental impacts. To address this concern, a detailed simulation and analysis was conducted for a hypothetical VVER-1200 nuclear reactor at Lake Kariba, focusing on a design basis loss of coolant accident (LOCA). The study utilized site-specific meteorological data for both the wet and dry seasons to model the dispersion of radioactive materials using the RASCAL 4.3.4 code. The health effects of the radiological accident were quantified using dosimetric quantities, specifically the Total Effective Dose Equivalent (TEDE) and Child Thyroid Committed Effective Dose (CTCED), which are crucial for evaluating the effectiveness of emergency mitigation actions such as evacuation, sheltering-in-place, and the administration of prophylactic potassium iodide (KI) as a thyroid blocking agent. The results revealed that the doses during the wet season were approximately three times higher than those in the dry season, with the maximum TEDE reaching 153 mSv at 0.16 km from the release point during the wet season, compared to 45.5 mSv during the dry season under the containment leakage release pathway. The study also showed that both TEDE and CTCED were significantly higher near the release point and decreased as the distance downwind increased. Beyond a radius of 16.09 km (10 miles) from the release point, doses fell below 1 mSv, making this region safe for the public except under the worst-case scenario during the wet season, where doses as high as 50.2 mSv were observed at the 16.09 km distance. These findings underline the need for robust emergency preparedness and response plans, tailored to the specific climatic conditions of the region. The study provides critical baseline data that can assist decision-makers and regulators in developing regulations and guidelines to ensure adequate protection of the public and the environment in the event of a radiological accident.

1. Introduction

The use of nuclear power plants produces minimal radioactivity in the atmosphere during normal operating conditions. However, their operation is significant in the event of an accident being sabotage, an attack or deliberate release into the atmosphere. These risks can severely impact public health and the environment, as evidenced by past nuclear accidents such as Fukushima (2011), Chernobyl (1986), and Three Mile Island (1979). These events, often caused by natural disasters, human error, or equipment malfunctions, result in the release of various radionuclides such as Cs-137, I-131 and Pu-239 (Hasegawa et al., 2015). These radioactive substances, which are produced by the fission of uranium or plutonium, can spread through the air as gases, aerosols, or particles, depending on their properties. For example, the Chernobyl disaster involved the release of a radioactive plume that dispersed across Europe, causing acute radiation sickness in onsite workers, with 28 fatalities within three months (WHO, 2020). Over 530,000 recovery workers were exposed to significant radiation doses, resulting in long-term health impacts. Zimbabwe, in its pursuit of economic growth, recognizes the importance of energy for development and aligns with the United Nations Sustainable Development Agenda 2030, advocating for affordable, sustainable, and modern energy (Nicholls, 2020). As part of this agenda, Zimbabwe may consider nuclear energy to meet its energy demands, emphasizing the need for a balanced energy mix to ensure long-term energy security (Nicholls, 2020). This research focuses on the atmospheric dispersion and dose assessment of a hypothetical

* Corresponding author.
E-mail address: chiyangwa.solomon01@gmail.com (S. Chiyangwa).

https://doi.org/10.1016/j.anucene.2025.111733
Received 23 March 2025; Received in revised form 19 June 2025; Accepted 8 July 2025
Available online 18 July 2025

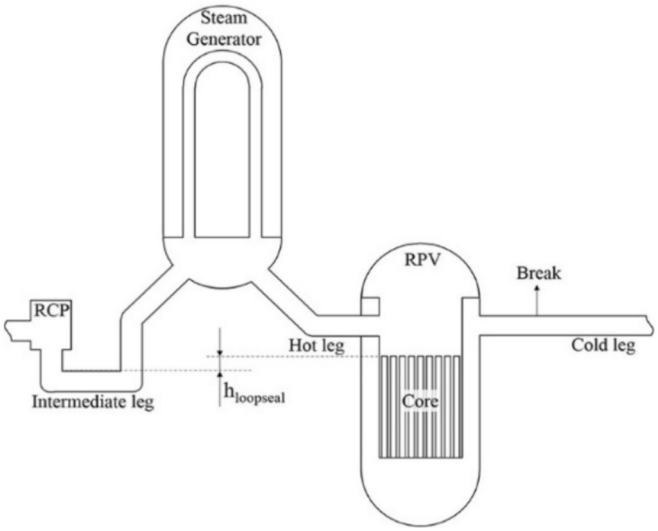

Fig. 1. Cold leg break leading to LOCA (Kim et al., 2020).

Loss of Coolant Accident (LOCA) scenario at a VVER-1200 nuclear plant in Zimbabwe, aiming to understand and mitigate the potential consequences of such events. Proper risk management, including radiation monitoring and emergency response, is essential to protect public health and minimize environmental harm. The research employed the Radiological System for Consequence Analysis (RASCAL) 4.3.4 code for assessment of radionuclide dispersion and the estimation of the Total Effective Dose Equivalent (TEDE) and the Child Thyroid Committed Effective Dose (CTCED). RASCAL is a widely used tool for radiological dose assessment in various scenarios, including nuclear accidents.

2. The postulated accident scenario and accident analysis

The radiological consequence analysis focused on a Design Basis Small Break – Loss of Coolant Accident (SB-LOCA) scenario involving a proposed VVER-1200 nuclear reactor, resulting in the release of radionuclides into the atmosphere. This LOCA scenario was attributed to a cold leg break in the primary coolant loop caused by flow-accelerated corrosion. LOCA conditions highlight the critical nature of this potential nuclear safety risk. It refers to a hypothetical event in which a breach in the primary coolant system or a failure in the reactor's cooling mechanisms prevents the coolant from reaching the reactor core. This loss of cooling can cause a rapid rise in fuel temperature, potentially resulting in fuel damage and the release of radioactive materials (Birikorang et al., 2025). The accident scenario under study helps to evaluate the performance of release mitigation systems, the proposed siting of the reactor and estimate the magnitude of the radiological health risk to the public. The LOCA scenario was selected over alternative scenarios because it serves as a standard benchmark in international nuclear safety guidelines. It is frequently referenced in IAEA safety report series No. 52 (IAEA, 2008), making it a common focus in global nuclear risk assessments and regulatory frameworks. Such safety assessments are integral to radiation protection protocols. This specific accident scenario is based on probabilistic safety assessment methods, thus identifying it as the primary contributor to the fission product class known as the source term category (STC). RASCAL 4.3.4 code was employed for simulating the postulated accident, enabling detailed analysis of the dispersion and impact of released radionuclides in the environment. Fig. 1 illustrates the structural components of the primary circuit in a Pressurized Water Reactor (PWR), highlighting the location of the breakage on the cold leg.

As illustrated in Fig. 1, the loss of coolant incident led to core degradation, which in turn caused the release of radionuclides into the reactor containment. Subsequently, these radionuclides escaped from the containment building into the atmosphere in both gaseous and particulate forms.

2.1. Hypothetical assumption for the LOCA

Below are the assumptions made for the accident scenario considered for the present work:

a. The reactor was operating at 1170 MW_e before the accident.
b. The accident was caused by a small cold leg break in the primary loop due to corrosion.
c. Functional failure of Emergency Core Cooling System (ECCS).
d. The release rate was 0.2 vol% / day at 52.2 m release height.
e. Reactor shutdown time, core uncovered, and core recovery time were 09:00, 11:00, and 13:00, respectively, for both wet and dry seasons.

2.2. Proposed reactor technical parameters

Table 1 presents a summary of the technical parameters of the proposed VVER-1200 reactor, which serve as the basis for simulating the design basis Loss of Coolant Accident (LOCA).

2.3. Proposed site of the reactor

Zimbabwe is a landlocked country, and therefore, the proposed site for the nuclear power plant (ZIMVVER1) considered in the simulation of the postulated accident is Lake Kariba. A lake created by constructing a dam wall across the Zambezi River in the Kariba Gorge, about 400 km

Table 1
Reactor technical parameters.

Reactor Parameter	Specification
Thermal capacity	3200.00 MW_{th}
Mean burn-up	60,000.00 MW/MTU
Containment type	PWR – dry containment
Containment volume	7.05×10^{04} m^3
Design Leak Rate	0.2 % volume/day
Coolant element	Light water
Primary coolant mass	2.36 x 10^5 kg
Assemblies of fuel	163
Steam generator type	U
Amount of steam generator water	52 220 Kg
Release height	52.2 *m*

Table 2
Pasquill-Gifford Scheme for Atmospheric Stability Classification.

Stability Class	Description
A	Extremely Unstable
B	Moderately Unstable
C	Slightly Unstable
D	Neutral
E	Slightly Stable
F	Moderately Stable
G	Very Stable

from Victoria Falls and it lies about 1300 Km upstream of the Indian Ocean, along the border between Zambia and Zimbabwe at −16°31′S 28°53′E and an elevation of 479 m. It spans more than 223 km in length and about 40 km in width. The Lake encompasses an area of 5580 square kilometers with a storage capacity of 185 cubic kilometers. According to the 2022 Population Census, Kariba town had a population of 27600.

2.4. Site meteorological conditions

The dispersion of released radionuclides in the atmosphere is affected by a range of meteorological factors, such as wind direction, wind speed, precipitation, and atmospheric stability class. The prevailing wind direction is reported to be at 240 degrees. Wind speeds in this region are typically below 8 knots (4.12 m/s), although occasional speeds above 13 knots (6.69 m/s) have been recorded. Data collected from the Meteorological Services Department of Zimbabwe spanning six years (2018–2023) indicate that wind speeds range from a minimum of 0.98 m/s to a maximum of 2.83 m/s. Generally, higher wind speeds are observed during the dry season, while lower speeds are noted during the wet season. The wet season spans from October to April, while the dry season spans from May to September. For the period under study (2018–2023), the average humidity over the selected site was 59.63 %. The lowest humidity readings were recorded during the dry season, and the wet season is dominated by high humidity.

The prevailing atmospheric stability class was D (Neutral). This is based on the Pasquil-Turner scheme (Turner, 1994). The Pasquill-Gifford scheme is a widely used method for classifying atmospheric stability, thus the behavioural pattern of the atmosphere, which helps in understanding how pollutants/radionuclides disperse in the atmosphere. It categorizes atmospheric conditions into stability classes ranging from A to G, which indicates the degree of turbulence and mixing of the air. Table 2 outlines the Pasquill-Gifford classification scheme used to describe atmospheric stability conditions, which are essential for modelling the dispersion of radioactive materials. Each stability class reflects different turbulence and mixing conditions in the atmosphere, often influenced by solar radiation, cloud cover, and wind speed. The associated wind speed ranges provide a general guideline for how each class interacts with local meteorological dynamics (Pasquill, 1961). These stability classes are integral to atmospheric dispersion models, such as those used in RASCAL 4.3.4, as they influence the rate and direction of contaminant spread. For instance, Class A conditions, characterized by strong surface heating and low wind speeds, lead to rapid vertical mixing, while Class F and G conditions result in limited dispersion, increasing the potential for localized dose accumulation (Turner, 1970).

The meteorological data were categorized into two distinct seasonal periods, the wet season and the dry season, as mentioned earlier. Table 3 presents a summary of the key meteorological parameters recorded at Lake Kariba. During the observation period, the dominant wind direction was 240 degrees, indicating that the prevailing winds primarily originated from the west-southwest.

The minimum, average, and maximum annual wind speeds for the two main seasons in Zimbabwe are presented to provide a better understanding of wind behaviour patterns, which are critical for accurate atmospheric dispersion modelling and effective emergency response planning in the event of a radiological release.

Table 4 presents the recorded wind speed data for the wet season in Zimbabwe over the six years from 2018 to 2023. This data provides insights into seasonal wind patterns, which are critical for assessing atmospheric dispersion behaviour and potential implications for emergency response planning.

Table 5 presents wind speed data recorded during the dry season in Zimbabwe from 2018 to 2023. This information is essential for understanding seasonal wind behaviour, which tends to be relatively light to moderate and more variable in direction. Such patterns are largely influenced by increased atmospheric moisture, frequent rainfall, and the dominance of low-pressure systems associated with the Intertropical Convergence Zone (ITCZ) (NOAA, 2023).

Although the difference in wind speeds between the wet and dry seasons was not statistically significant, a slight decrease in average

Table 4
Average wind speeds during the wet season (2018–2023).

Year	Wind Speed (m/s)		
	Min	Average	Max
2018	0.98	1.49	2.47
2019	1.39	1.80	2.52
2020	1.13	1.75	2.62
2021	0.98	1.34	2.01
2022	0.87	1.44	2.26
2023	1.13	1.44	2.06
Annual Average	**1.08**	**1.54**	**2.31**

Table 5
Average wind speeds during the dry season (2018–2023).

Year	Wind Speed (m/s)		
	Min	Average	Max
2018	1.08	1.80	2.83
2019	1.70	2.11	2.57
2020	1.39	1.85	2.62
2021	1.08	1.44	1.90
2022	1.13	1.65	2.83
2023	0.98	1.34	1.80
Annual Average	**1.23**	**1.70**	**2.42**

Table 3
Average Meteorological Data for the Kariba area in Zimbabwe.

Year	Prevailing Wind Direction	Wind Speed (m/s)			Stability Class	Relative Humidity (%)
		Average	Min	Max		
2018	240	1.62	0.98	2.83	D	66.58
2019	240	1.93	1.39	2.57	D	55.08
2020	240	1.79	1.13	2.62	D	59.67
2021	240	1.38	0.98	2.01	D	60.58
2022	240	1.52	0.87	2.83	D	57.67
2023	240	1.39	0.98	2.06	D	58.21
Annual Average		**1.61**	**1.05**	**2.49**		**59.63**

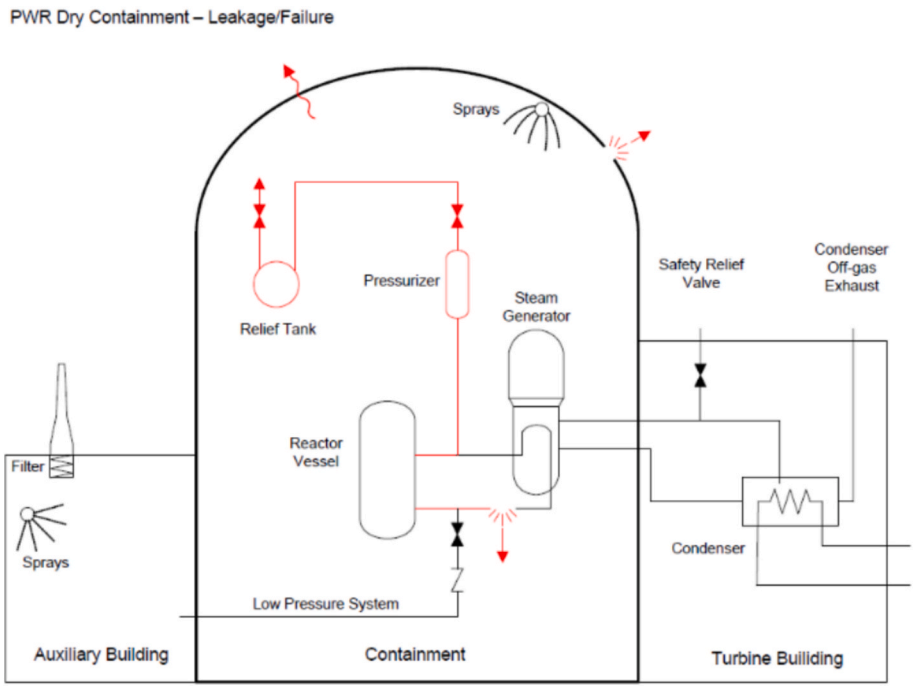

Fig. 2. Containment Leakage/Failure Release Pathway Modeled in RASCAL (Ramsdell et al., 2013).

Table 6
Meteorological data used for the simulation of the LOCA under study.

Parameter	Wet Season	Dry Season
Wind speed	(1.1, 1.5 and 2.3)	(1.2, 1.7 and 2.4)
Humidity	63.9	53.6
Precipitation	Rain	No Precipitation
Stability Class	(A, D and G)	(A, D and G)

wind speed was observed during the wet season. This minor variation is influenced by several interconnected atmospheric and environmental factors. These include differences in atmospheric pressure systems, temperature gradients, land surface characteristics such as vegetation cover and land use, as well as broader regional climate patterns.

During the dry season, stronger and more sustained winds are typically observed. This is largely due to more pronounced temperature gradients, reduced surface roughness, and the influence of high-pressure systems, all of which enhance wind flow. In contrast, the wet season is generally associated with weaker and more variable wind patterns. The slightly lower wind speeds during this period can be attributed to increased atmospheric moisture, frequent rainfall, and greater cloud cover, which collectively reduce surface heating. Additionally, the dominance of low-pressure systems such as the Intertropical Convergence Zone (ITCZ), diminished temperature gradients, and increased vegetation growth further contribute to calmer and less consistent wind conditions (UN Climate Report, 2022).

2.5. Release pathway

The RASCAL 4.3.4 code is designed to simulate the radiological consequences of nuclear incidents by modeling three primary release pathways: containment bypass, steam generator tube rupture, and containment leakage or failure. In the context of the accident scenario analyzed in this study, containment leakage or failure was determined to be the most appropriate release pathway.

This selection is based on the nature of the postulated event, a severe LOCA, during which the rapid loss of reactor coolant leads to overheating of the reactor core. As the fuel rods are exposed to high-temperature steam, an intense exothermic zirconium-steam reaction occurs, resulting in significant hydrogen generation and pressurization within the containment structure. These conditions may compromise the integrity of the containment, leading to a widespread release of radionuclides into the environment. This scenario is representative of a worst-case outcome and is consistent with the conditions that RASCAL is designed to evaluate for emergency response and consequence analysis. Fig. 2 shows a snapshot from the RASCAL 4.3.4 user interface, illustrating the reactor configuration and indicating the specific location where radionuclides are released into the atmosphere.

2.6. Simulation using rascal 4.3.4 code

The RASCAL 4.3.4 software is utilized by the Protective Measures Team at the US Nuclear Regulatory Commission's Operations Center. It helps generate independent dose and consequence projections during radiological incidents and emergencies. Developed to quickly assess incidents or accidents at facilities licensed by the US Nuclear Regulatory Commission, the tool supports decision-making processes, such as determining if the public should evacuate or take shelter. The code provides a first-order approximation of the radiation impacts linked to the atmospheric release of radioactive materials (Ramsdell et al., 2013). RASCAL 4.3.4 is a comprehensive modeling system for assessing the

Table 7
Recommended protective actions (U.S. EPA, 2017).

Phase	Protective Action Recommendation	PAG Limit [mSv]	Comments
Early Phase	**Sheltering-in-place**	four days)	The total projected dose by external exposure and the committed effective dose for internal exposure for 4 days
	Evacuation of the public		
	Administration of prophylactic drugs- Potassium Iodide (KI)	50 (received on the thyroid by a child's exposure to iodine)	After the approval of the medical team

consequences of radiological releases from nuclear reactors and other facilities (USNRC, 2012). The code includes modules for atmospheric dispersion modeling, dose assessment, and emergency response support. It is suitable for a wide range of radiological scenarios and regulatory applications. RASCAL 4.3.4 code applies a straight-line Gaussian plume model for areas close to the source where travel times are short and dry deposition has minimal impact. For longer distances where changes in meteorological conditions and dry deposition effects become more pronounced, the RASCAL 4.3.4 code transitions to a Lagrangian-trajectory Gaussian puff model. This unique feature sets RASCAL 4.3.4 apart from other codes, contributing to the accuracy of dose estimation results (US EPA, 2016).

Meteorological data were obtained from the Meteorological Services Department of Zimbabwe, and relevant technical specifications of the proposed VVER-1200 reactor were documented using various literature. The meteorological data were categorized into two main seasons—wet and dry—and further organized to reflect average, minimum, and maximum wind speeds recorded over a six-year period (2018–2023), as presented in Tables 4 and 5. To represent these seasonal variations in the simulation, January 10, 2024, was selected to characterize the wet season, while August 10, 2024, was chosen to represent the dry season. Simulations were conducted using average, minimum, and maximum wind speeds to estimate dispersion patterns and resulting radiological doses. The RASCAL 4.3.4 code was employed to calculate the source term required for modeling the Loss of Coolant Accident (LOCA) scenario under investigation. This calculation was based on the time intervals during which the reactor core was assumed to be uncovered, in combination with the meteorological data and reactor parameters.

The simulation was carried out to assess the dispersion and radiological impact of key radionuclides, Cs-137, I-131, and Xe-133, from a nuclear release point. Each radionuclide was selected based on its radiological significance and mode of exposure: Cs-137 was analyzed for groundshine exposure, I-131 for inhalation dose, and Xe-133 for cloudshine effects. These radionuclides were chosen due to their distinct physical characteristics, radiological behaviours, and varying health impacts over time. Notably, Cs-137 and I-131 are beta-emitting isotopes known to cause localized tissue damage upon inhalation, ingestion, or dermal contact (Birikorang et al., 2025). The primary objective of the simulation was to estimate radiation doses from inhalation, cloudshine, and groundshine exposure pathways under accident conditions. A worst-case scenario was modelled, simulating a nighttime accident during the wet season to determine the Total Effective Dose Equivalent (TEDE). To maximize deposition and evaluate the most severe consequences, the simulation incorporated Stability Class G, representing highly stable atmospheric conditions, a prolonged core recovery time of 4 h, and a minimum seasonal wind speed of 1.1 m/s, characteristic of the wet season as presented in Table 6.

The RASCAL 4.3.4 simulation procedure was initiated by selecting the primary tool, the source term to dose (STDose) tool. The system now becomes activated, after which the user specifies the location of the event and the type of incident that has occurred, such as (Table 7) a reactor accident or radiological release scenario. Once the event type is defined, all relevant reactor parameters are inputted to provide essential technical details about the facility involved. This information, combined with the event data, allows RASCAL to generate the source term, which represents the quantity and characteristics of the radionuclides expected to be released. The simulation also requires the user to define the release path, indicating how the radioactive material exits the containment or reactor system, whether through a stack, valve, or structural breach. In addition, accurate meteorological data is supplied, including wind speed, wind direction, atmospheric stability class, and precipitation levels, all of which are critical for modelling atmospheric dispersion. With the source term, release path, and weather data in place, the system proceeds to perform dose calculations, estimating radiation exposure levels at various distances from the release point. The outcome of the simulation is usually a set of detailed results that describe the projected radiological consequences or the proposed scenario, including dose distributions and concentration profiles. The procedure concludes with the end of the simulation process, providing emergency responders and decision-makers with critical information to support protective action recommendations and public safety measures. Fig. 3 presents the flow chart diagram illustrating the RASCAL 4.3.4 simulation process carried out during the study.

Upon obtaining results for the Total Effective Dose Equivalent (TEDE) and the Child Thyroid Committed Effective Dose (CTCED), a comparison was made between these two release pathways considered

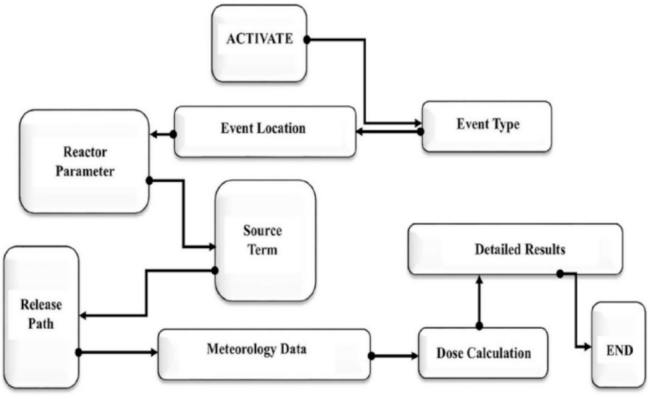

Fig. 3. Flow Chart diagram of RASCAL 4.3.4 simulation process (Birikorang et al., 2025).

Table 8
Summary of activity released to the atmosphere.

Containment Leakage/Failure		
Radionuclide Group	Activity (Bq)	% of Total Activity
Noble Gas	9.50×10^{14}	70.5
Iodines	3.10×10^{14}	22.7
Other	9.20×10^{13}	6.8
Total	$\mathbf{1.35 \times 10^{15}}$	**100**

in the simulation. Furthermore, the TEDE and the CTCED were compared to the EPA limits for protective action intervention (U.S. EPA, 2017), at the early phase of the release. The protective actions examined in this current study were sheltering, evacuation, and Supplementary administration of prophylactic drugs – potassium iodide (KI). Table 6 presents the protective actions for the early phase of a radiological accident based on the U.S. EPA 2017.

In estimating radiation doses, the RASCAL 4.3.4 code alternates between two atmospheric dispersion models: the Straight-Line Gaussian Plume Model and the Lagrangian Trajectory Gaussian Puff Model. The Gaussian Plume Model, one of the most extensively validated in the field of atmospheric dispersion, has been applied across various domains (Cao et al., 2016). It is particularly suitable under conditions where key meteorological variables, such as wind speed, wind direction, atmospheric turbulent diffusivity, and pollutant emission rate, remain constant over time.

The Plume Model utilizes a polar grid system comprising receptors arranged in eight concentric circles, with receptor points located at 10-degree intervals around each circle. It operates under a steady-state

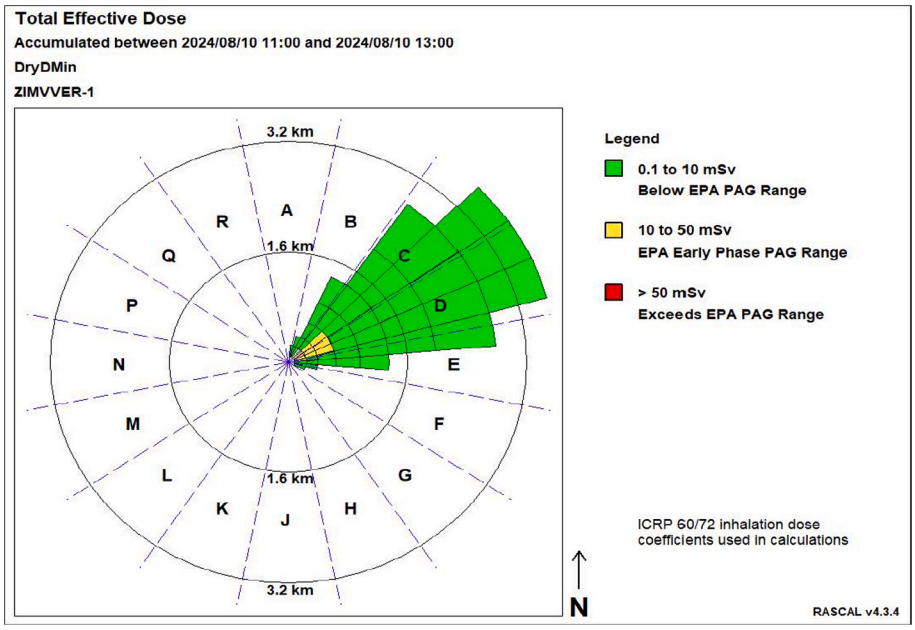

Fig. 4. Dose footprint of TEDE showing the direction of propagation in the dry season.

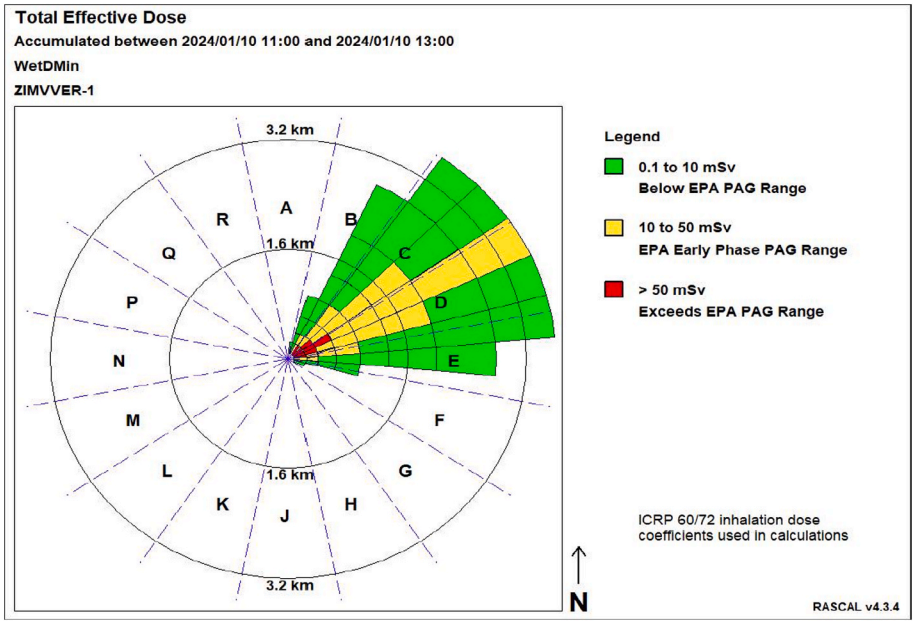

Fig. 5. Dose footprint of TEDE showing the direction of propagation in the wet season.

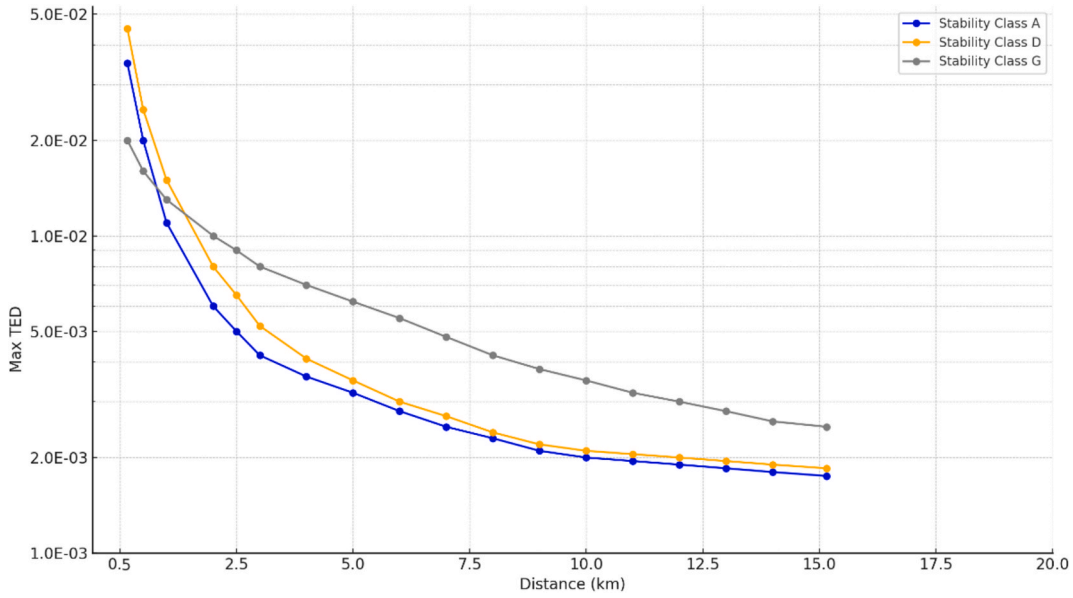

Fig. 6. Variation of TEDE with distance from the release point – Dry Season.

assumption, meaning the released material is instantaneously dispersed across all downwind distances. The concentration at any point within the plume is determined by summing the contributions of all overlapping puffs at that location. The Gaussian Puff Model assumes meteorological conditions are constant over the puff's trajectory. When the wind speed is sufficiently high and the receptor is positioned far downwind, such that changes in dispersion parameters along the puff's path are negligible, the puff model effectively simplifies into the plume model (Ramsdell et al., 2013). The average concentration during the passage of the plume can then be estimated using a standard Gaussian dispersion equation, assuming the x-axis aligns with the prevailing wind direction, as shown in Eq. (1) below.

$$X(x,y,z) = \int_{t=-\infty}^{t=\infty} \frac{Q' F_y F_z}{(2\pi)^{3/2}\sigma_x(x)\sigma_y(x)\sigma_z(x)} \exp\left[-0.5\left(\frac{x-ut}{\sigma_x(x)}\right)^2\right] d_t \quad (1)$$

x is the average concentration of radionuclides at a point (x,y,z), σ_y and σ_z are the standard deviations of the pollutant distribution in the lateral (y) and vertical (z) directions respectively, F_y and F_z are vertical and lateral exponential terms, given by $\exp\left[-0.5\left(\frac{y-y_0}{\sigma_y}\right)^2\right]$ and $\exp\left[-0.5\left(\frac{z-z_0}{\sigma_z}\right)^2\right]$ respectively. Q' is the release rate, u is the wind speed and t is time. According to the principle of superposition, the one-dimensional solution to the diffusion equation can be extended, leading to the creation of the fundamental Gaussian puff model. In a Cartesian coordinate system where x and y are in the horizontal plane and z is vertical, the normalized concentration X in the Gaussian Puff Model is expressed by the Eq. (2) below.

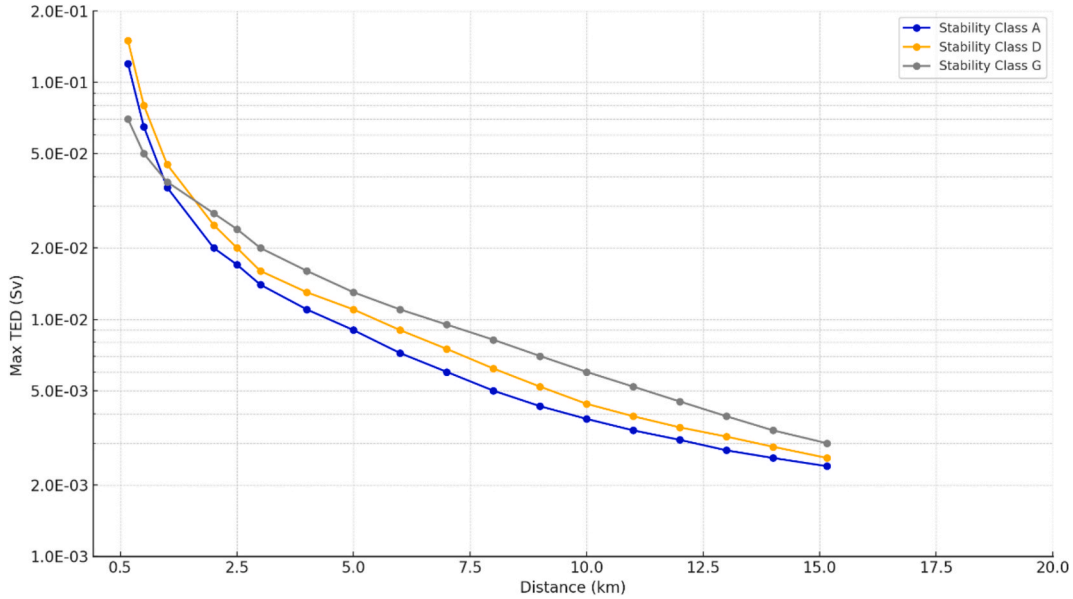

Fig. 7. Variation of TEDE with distance from the release point – Wet Season.

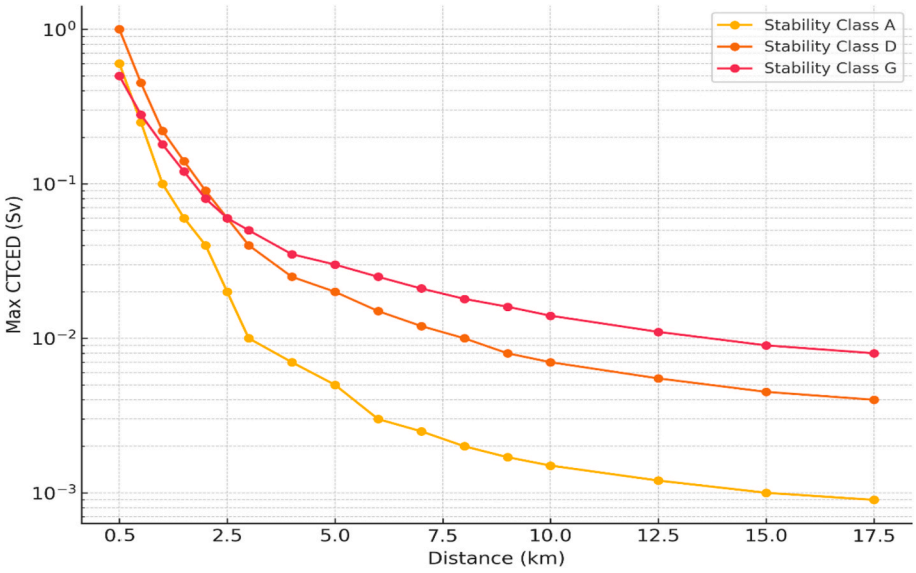

Fig. 8. Variation of CTCED with Distance during the Wet Season.

$$\frac{X(x,y,z)}{Q} = \frac{1}{(2\pi)^{3/2}\sigma_x\sigma_y\sigma_z}\exp\left[-0.5\left(\frac{x-x_0}{\sigma_x}\right)^2\right]\exp\left[-0.5\left(\frac{y-y_0}{\sigma_y}\right)^2\right]\exp\left[-0.5\left(\frac{z-z_0}{\sigma_z}\right)^2\right] \quad (2)$$

Q is the release rate and X is the concentration of radionuclides at a point (x, y, z).

3. Results and discussion

The results are from the simulation of a design-basis LOCA for a hypothetical VVER-1200 nuclear reactor using the RASCAL 4.3.4 code. The discussed results include TEDE, CTCED, and the recommended protective actions for Zimbabwe's two main seasons: the wet and dry seasons.

3.1. Source term generation using rascal

The RASCAL code was used to generate the source term for the accident scenario. Table 8 shows the categories of radionuclides released for the containment leakage pathway.

3.2. Plume direction of propagation for TEDE

The RASCAL 4.3.4 code was employed to simulate dose footprints, illustrating the directional movement of the radioactive plume. The dominant plume trajectory was observed to be toward the northeast. Simulation results indicated that radionuclide deposition was significantly higher during the wet season, primarily due to enhanced wet deposition processes. A comparative analysis of the dose footprints revealed that TEDE values extended over a wider area from the release point in the wet season than in the dry season. This observation is attributed to a combination of factors, which include atmospheric dispersion, wet deposition, resuspension, and surface run-off. To better

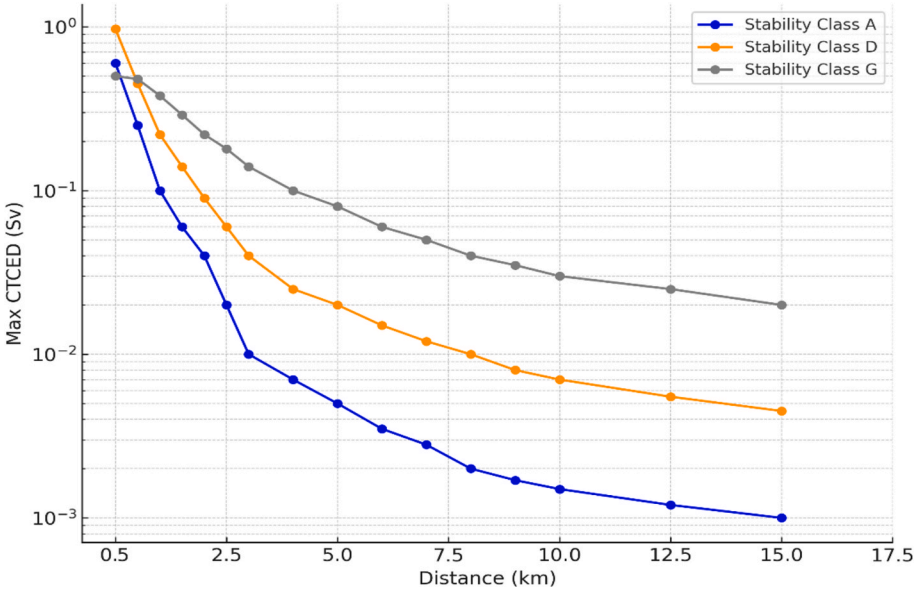

Fig. 9. Variation of CTCED with Distance during the Dry season.

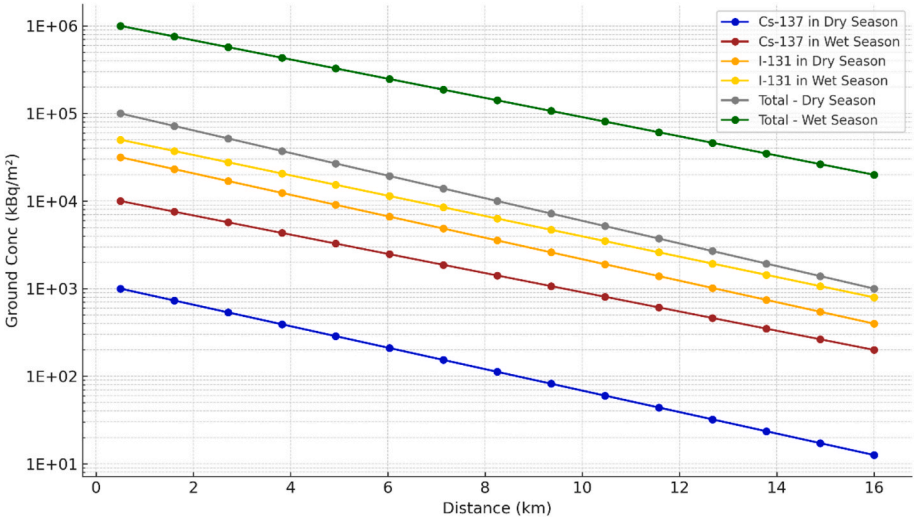

Fig. 10. Ground Concentration (Surface Concentration) during the Wet Season.

understand plume behavior in relation to TEDE, dose footprints corresponding to the prevailing atmospheric stability class D were generated using RASCAL. Figs. 4 and 5 present the resulting dose footprints for the dry and wet seasons, respectively, based on the containment leakage release pathway.

In Fig. 4, the simulation output presents a comprehensive image of the TEDE distribution resulting from a hypothetical radiological release scenario at the ZIMVVER-1 reactor. Using a polar coordinate grid, the output illustrates radiation exposure levels covering up to 3.2 km from the release point. The diagram classifies the affected areas into three dose zones: the green zone (0.1–10 mSv), representing regions with radiation levels below the U.S. EPA PAG threshold for early-phase response and indicating minimal radiological risk; the yellow zone (10–50 mSv), which falls within the EPA early-phase PAG range and denotes areas where protective actions such as sheltering or evacuation may be necessary; and the red zone (greater than 50 mSv), which exceeds the EPA-PAG limits and signifies severe radiological hazards requiring immediate intervention. The plume distribution, predominantly affecting sectors B, C, D, and E, reflects the influence of prevailing wind patterns on atmospheric dispersion. This highlights the essential role of real-time meteorological data in emergency response planning. The dose estimations are based on ICRP 60/72 inhalation dose coefficients, providing a uniform approach to radiological risk assessment. From the figure, while most of the impacted region lies within the green zone, indicating lower exposure, portions of the area extend into the yellow, which falls within the EPA early-phase PAG range, recommended for sheltering and evacuation.

Fig. 5 illustrates an overlap between the yellow and red zones as compared to Fig. 4 within the dose distribution map. This indicates that certain areas are receiving more radiation doses that exceed the U.S. EPA-PAG thresholds for the early phase of a radiological emergency. The red zone dose levels exceed the 50 mSv, surpassing the upper limit of the EPA's early phase PAG range. The presence of such elevated dose levels suggests that the affected areas are experiencing radiation intensities beyond the acceptable limits for public exposure. This presents a significant radiological hazard and calls for immediate protective measures, such as evacuation or shelter-in-place directives.

3.3. Variation of TEDE with distance from the release point

The simulation results show that the TEDE decreases with increasing distance from the release point. The lower radiation doses downwind are due to dilution and dispersion of the released radionuclides. Using minimum speed (1.1 ms^{-1} and 1.2 ms^{-1} for the wet and dry seasons, respectively) for maximum deposition, Figs. 6 and 7 were plotted to show the relationship between TEDE and distance from the release point at different stability classes during the dry and wet seasons. It was observed that under stability class G, the TEDE initially increased before decreasing sharply. In contrast, the TEDE values for stability classes A and D exhibited a consistent decreasing trend throughout the simulation.

The simulation showed an interesting pattern under stability class G, where the radiation dose rose and dropped sharply. This happened because class G represents very calm atmospheric conditions where there is hardly any vertical or horizontal air movement. That means the radioactive plume does not spread out much. Instead, it lingers and stays concentrated near the release point. As a result, people or objects close to the source would experience higher radiation doses. But as the plume moves away from the source, it either slowly disperses or settles closer to the origin, leading to a significant drop in dose levels further out.

On the other hand, the radiation dose under stability classes A and D followed a steady downward trend from the beginning. This is because class A usually occurs during hot daytime conditions that cause strong air movement and mixing, while class D is linked with overcast skies or gentle winds, which help spread the plume more evenly. These conditions allow the radioactive material to disperse more broadly, lowering its concentration in any one place. As a result, TEDE values remain relatively low and continue to decrease the farther the plume travels from the source.

Table 9
PAGs and protective actions – wet season.

Site	Maximum Dose [mSv] Distance [km]	PAG [mSv]	Impact Area [km^2]	Maximum Distance Reached [km] Dose [mSv]	Recommended Protective Action
(Prevailing Wind Direction = 240 deg)	153(0.16)	50	0	(0.48)52.0	Evacuation to 0.48 km
		10	0.1	(3.22)10.4	Sheltering to 3.22 km
		0.1	3.8	(16.09)2.93	Safe area from 3.22 km

Table 10
PAGs and Protective Actions – Dry season.

Site	Maximum Dose [mSv] Distance [km]	PAG [mSv]	Impact Area [km^2]	Maximum Distance Reached [km] Dose [mSv]	Recommended Protective Action
(Prevailing Wind Direction = 240 deg)	45.5(0.16)	50	0	N/A	N/A
		10	0	(0.48)13.9	Sheltering to 0.48 km
		0.1	1.9	(16.09)0.29	Safe area from 0.48 km

Table 11
PAGs and Protective Actions for the Wet Season.

Site	Maximum Dose [mSv] Distance [km]	PAG [mSv]	Impact Area [kmˆ2]	Maximum Distance Reached [km]Dose [mSv]	Recommended Protective Action
(Prevailing Wind Direction = 240 deg)	994(0.16)	250	0	(0.48)295	KI admission for adults up to 40 yearsfor under 0.48 km
		50	0	(1.61) 65.50	KI admission for children, pregnant and lactating womanfor under 1.61 km
		0.5	3.7	(16.09) 6.42	Safe area from 1.61 km

3.4. Comparison of results for the simulation scenarios based on CTCED

The RASCAL 4.3.4 code computed the Child Thyroid Committed Effective Dose (CTCED) for the simulated hypothetical accident scenario. The analysis of CTCED was pivotal for the demarcation of emergency zones and the suggestion of recommended protective actions regarding the administration of prophylactic KI to limit the uptake of radioactive iodine. It was noted that the CTCED decreased with an increase in distance from the release point for all three atmospheric stability classes used in this study. Stability Class G dominated downwind with wet season doses slightly higher than the dry season. Using the minimum wind speed for maximum deposition under the prevailing stability D, the maximum CTCED was 9.73 x 10^{-01} Sv during the dry season and 9.94 x 10^{-01} Sv for the wet season.

The slight difference is due to wet deposition, which reduces the amount of iodine that remains available for inhalation as compared to the dry season. Figs. 8 and 9 show the relationship between CTCED and distance from release under different atmospheric stability classes for the wet and dry seasons, respectively.

3.5. Ground concentration of radionuclide emission

The results presented reflect the ground-level concentrations of radionuclides Cs-137 and I-131, with Xe-133 excluded from the analysis due to its negligible contribution to ground deposition. A comparative assessment was conducted between the total ground concentration and the individual concentrations of Cs-137 and I-131 under both wet and dry seasonal conditions, using the prevailing atmospheric stability class D. To ensure a representative scenario for maximum deposition, the average wind speed for the site was employed in the simulation. The findings indicate that ground-level concentrations were significantly higher during the wet season compared to the dry season. This suggests that precipitation plays a major role in enhancing radionuclide deposition on the ground, thereby increasing potential radiological impact during wet conditions. The highest total ground concentration during the wet season was at 0.16 km with a concentration value of 9.22 $\times$ 10^{05} kBq/m^2. The maximum ground concentration of Cs-137 and I-131 were 4.85 $\times$ 10^{04} kBq/m^2 and 8.77 x 10^{04} kBq/m^2 respectively, all at 0.16 km distance from the release point. Both values were recorded during the wet season. The ground concentration was observed to be decreasing as the distance from the release point increased. Fig. 10 shows the graphical representation of the ground concentration for the wet season for the radionuclides.

3.6. Recommended protective actions based on TEDE

This section outlines suggested protective measures in response to a hypothetical nuclear accident scenario. The guidance follows the early-phase Protective Action Guides (PAGs) provided by the U.S. Environmental Protection Agency (EPA). These recommendations are informed

Table 12
PAGs and Protective Actions for the Dry season.

Site	Maximum Dose [mSv] / Distance [km]	PAG [mSv]	Impact Area [km^2]	Maximum Distance Reached [km] / Dose [mSv]	Recommended Protective Action
(Prevailing Wind Direction = 240 deg)	973/(0.16)	250	0	(0.48)/296	KI admission for adults up to 40 yearsfor under 0.48 km
		50	0	(1.61)/63.50	KI admission for children, pregnant and a lactating motherfor under 1.61 km
		0.5	3.1	(16.09)/5.92	Safe area from 1.61 km

Table 13
Early Phase Protective Actions for the worst-case scenario.

Site	Maximum Dose [mSv] / Distance [km]	PAG [mSv]	Impact Area [km^2]	Maximum Distance Reached [km] / Dose [mSv]	Recommended Protective Action
(Prevailing Wind Direction = 240 deg)	833/(0.16)	50	0.2	(4.83)/50.20	Evacuation to 4.83 km
		10	1.3	(16.09)/25.7	Sheltering to 16.09 km
		0.1	3.6	N/A	Safe area from 16.09 km

by dose assessments generated from simulations carried out under atmospheric stability class D conditions—a common weather pattern that can influence how radioactive materials spread.

To reflect seasonal differences in environmental conditions, two sets of protective actions have been developed. Table 9 shows the recommended actions for the wet season, while Table 10 presents those tailored for the dry season. These recommendations aim to help protect public health by guiding early decision-making during a nuclear emergency.

The simulation results showed that the wet season recorded significantly higher Total Effective Dose Equivalent (TEDE) values near the release point compared to the dry season. Specifically, the peak TEDE during the wet season reached 153 mSv, whereas the dry season recorded a peak of 45.5 mSv. This difference also influenced the location of the safe zone boundary; during the dry season, the zone began as close as 0.48 km from the release point, while in the wet season, it started farther away at 3.22 km. The higher radiation dose during the wet season can largely be explained by the effect of wet deposition. When it rains, airborne radioactive particles are captured by raindrops and brought down to the ground more efficiently than in dry conditions. This process, known as scavenging, causes radionuclides to accumulate more rapidly and in higher concentrations on surfaces, leading to elevated radiation levels near the source (Keller et al.,1982; IAEA, 2018). In contrast, during the dry season, the absence of rain allows for greater atmospheric dispersion and slower ground-level accumulation, resulting in lower radiation exposure.

3.7. Recommended protective actions based on CTCED

The RASCAL code estimates the amount of radioactive iodine absorbed by children's thyroids to help decide what protective actions are needed, since children are especially vulnerable and have heightened sensitivity to radioactive iodine. But it's important to remember that adults and breastfeeding mothers also need protection. That is why this study includes clear potassium iodide (KI) guidelines for these groups, following advice from trusted health organizations like the WHO, IAEA, and CDC, so everyone at risk can be properly cared for during an emergency.

This refers to the administration of KI to block the uptake of radionuclides as a supplementary protective action. The prevailing stability D was selected to recommend protective actions. Tables 11 and 12 represent the early phase protective actions for the wet and dry seasons (Table 13).

No significant difference was found in the doses for the wet and dry seasons. In both cases, the safe area started at the same distance from the release point (1.61 km). This distance is very close to the release point, indicating minimal chances of encountering exposure in terms of CTCED. However, a higher impact area was recorded during the wet season than the dry season, and this is attributed to wet deposition, resuspension and run-off.

3.8. The worst-case scenario

The TEDE for the worst-case scenario was six times larger than the normal accident. The normal accident had a maximum TEDE of 0.128 Sv, whereas the worst-case scenario had a maximum of 0.83 Sv. As a result of elevated doses, the safe area was beyond 16.09 km.

4. Conclusion

This study looked at a small leak accident at a hypothetical nuclear power plant near Lake Kariba, Zimbabwe, using the RASCAL 4.3.4 simulation tool. It found that xenon-133 was released the most into the air, while iodine-131 settled the most on the ground, posing a bigger health risk than cesium-137. The radioactive cloud mainly moved northeast, mostly affecting areas within Zimbabwe. Radiation dose levels were at their highest close to the release point and dropped quickly further away. Most radiation doses were below the acceptable safety limits set by the regulatory commissions. But areas very close to the plant, up to about half a kilometer in the dry season and over 3 km in the wet season, needed emergency actions like sheltering or evacuation. Children within 1.6 km would need potassium iodide tablets to protect their thyroids. In the worst wet-season scenario, people had to shelter as far as 16 km away. This study shows how weather and seasons play a big role in planning for nuclear emergencies and protecting people effectively.

Declaration of competing interest

The authors declare that they have no known competing financial interests or personal relationships that could have appeared to influence the work reported in this paper.

Acknowledgements

I would like to thank the author and finisher, the Almighty God, for the successful compilation of my research work. Special thanks go to Dr. Birikorang and Prof. Agbodemegbe, who, despite their many duties, agreed to help me in carrying out the study. Many thanks to the IAEA for affording me such a precious opportunity to further my studies. Lastly, I sincerely express my heartfelt gratitude to my family and friends for their indefatigable support.

Data availability

Data will be made available on request.

References

Birikorang, S.A., Dahunsi, S., Adu, S., Nketia, C.A., Blay, A., 2025. Assessing nuclear energy and radiological risks: a case study of radionuclide dispersion from potential nuclear power plant accidents in Ghana. Radiat. Prot. Dosim. https://doi.org/10.1093/rpd/ncaf024.

Cao, B., Zheng, J., Chen, Y., 2016. Radiation dose calculations for a hypothetical accident in xianning nuclear power plant. Sci. Technol. Nucl. Installations.

Hasegawa, A., Tanigawa, K., Ohtsuru, A., Yabe, H., Maeda, M., & Shigemura, J. (2015). Health effects of radiation and other health problems in the aftermath of nuclear accidents, with an emphasis on Fukushima.

IAEA. (2008). Best Estimate Safety Analysis for Nuclear Power Plants: Uncertainty Evaluation (Safety Reports Series No. 52). International Atomic Energy Agency.

IAEA. (2018). *Modelling Radiological Consequences of Nuclear Accidents for Emergency Preparedness and Response*. IAEA Safety Reports Series No. 104. Vienna: IAEA.

Keller, J. H., Hoffman, L. G., & Voillequé, P. G. (1982). Wet Deposition Processes for Radioiodines (NUREG/CR-2438, ENICO-1111). Exxon Nuclear Idaho Company, Inc., and Science Applications, Inc., Idaho National Engineering Laboratory.

National Oceanic and Atmospheric Administration (NOAA). (2023). Inter-Tropical Convergence Zone. U.S. Department of Commerce.

Nicholls, A., 2020. Sustainable energy for development: a global perspective. Renew. Energy J. 25 (2), 110–125.

Pasquill, F., 1961. The estimation of the dispersion of windborne material. Meteorol. Mag. 90, 33–49.

Ramsdell, J. V., Athey, G. F., & Rishe, J. P. (2013). RASCAL 4.3 Workbook. Prepared for the Office of Nuclear Regulatory Research, U.S. Nuclear Regulatory Commission, Washington, DC.

Turner, D. B. (1970). Workbook of Atmospheric Dispersion Estimates. U.S. Department of Health, Education, and Welfare, Public Health Service, Environmental Health Service, Public Service Publication No. 999-AP-26, EPA 742-R-70-001.

Turner, D. B. (1994). *Workbook of Atmospheric Dispersion Estimates: An Introduction to Dispersion Modeling* (2nd ed.). CRC Press.

U.S. Environmental Protection Agency (EPA) (2017). Protective Action Guides and Planning Guidance for Radiological Incidents (EPA-400/R-17/001). U.S. Environmental Protection Agency. https://www.epa.gov/sites/default/files/2017-01/documents/epa_pag_manual_final_revisions_01-11-2017_cover_disclaimer_8.pdf.

UN Climate Report, 2022. Understanding wind patterns and their seasonal changes. United Nations. Clim. Change.